Supplementary information for

Improved Catalytic Effect and Metal Nanoparticle Stability using Graphene Oxide Surface Coating and Reduced Graphene Oxide for Hydrogen Generation from Ammonia-Borane Dehydrogenation

Samikannu Prabu and Kung-Yuh Chiang

Graduate Institute of Environmental Engineering, National Central University, Tao-Yuan, 32001, Taiwan

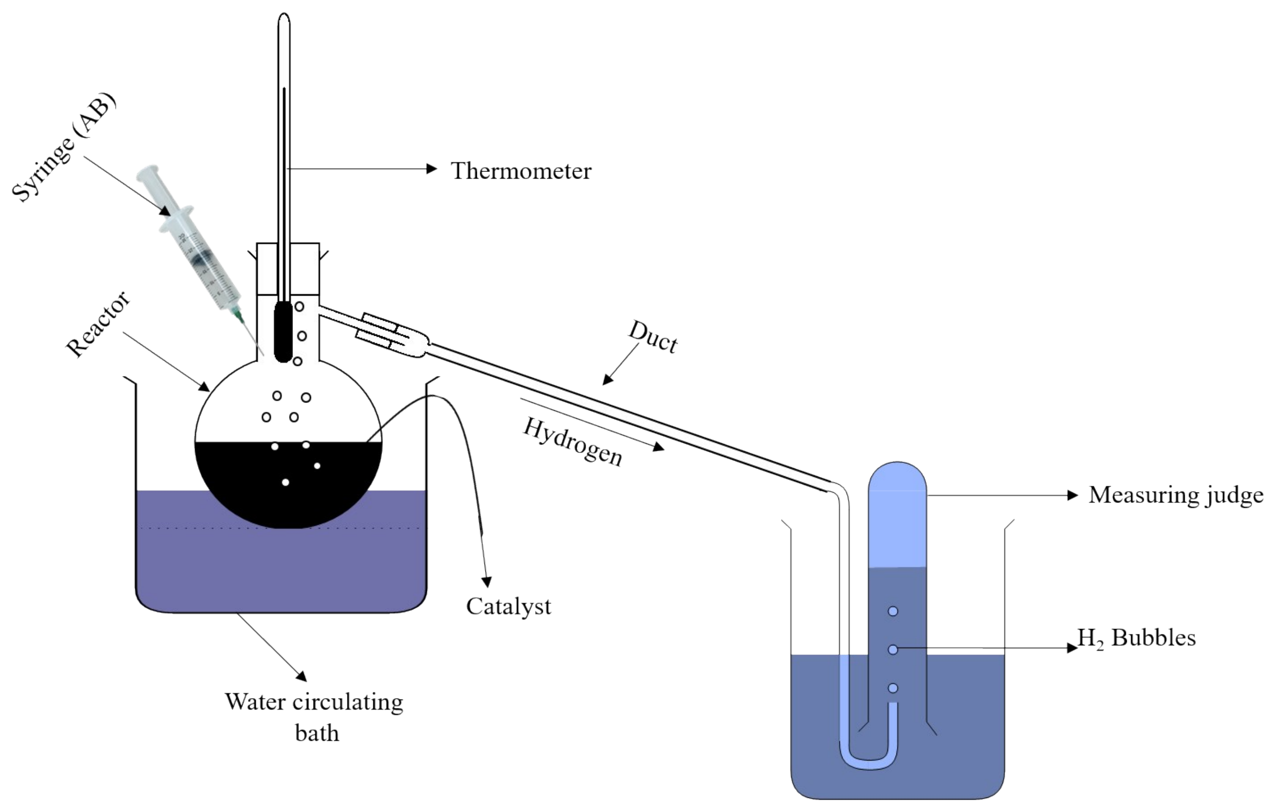

SFig. 1 Experimental setup for aqueous AB solution hydrolysis.

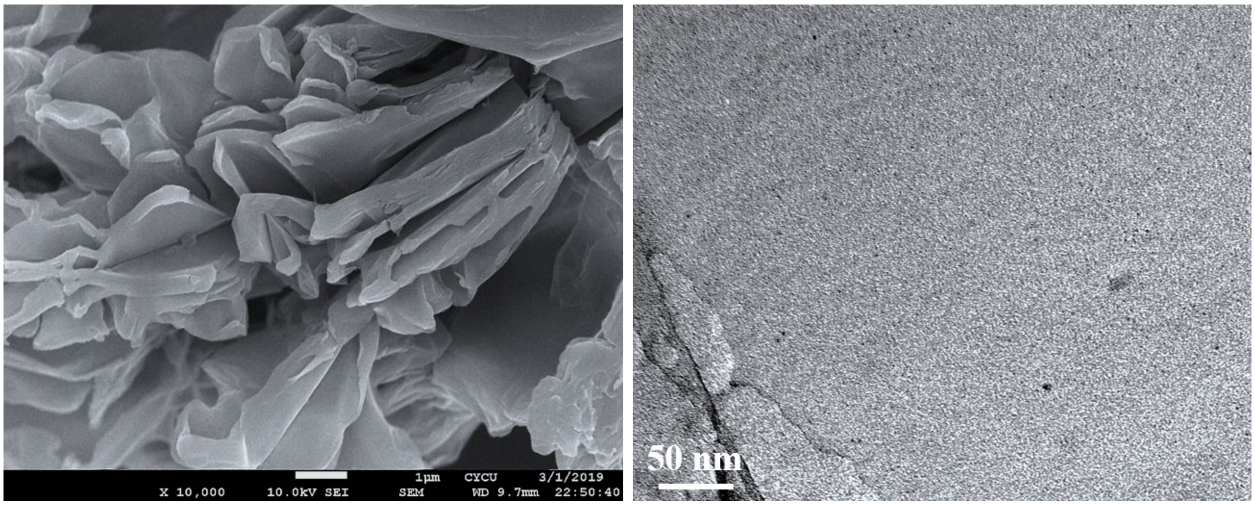

SFig. 2 SEM and TEM images of graphene oxide (GO).

SFig. 2 shows the FESEM image of as-synthesized GO and note that distinctly separated flakes with small corners are developed. The GO Nano-sheet shows a closely crowded lamellar structure and a smooth surface, with shiny multilayered microstructure. The GO samples contain several layers of aggregated and square-shaped crumpled sheets closely associated with each other to form a continuous conducting network. Through the exfoliation of graphite into GO, the edges of the GO sheets become creased, folded, and closely restacked, and the GO surface exhibits a soft carpet-like morphology, because of the presence of residual H_2O molecules and hydroxyl or carboxyl groups. In contrast to GO, the GO sheet exhibits transparent swelled silk-like waves or a flaky, scale-like, layered structure.

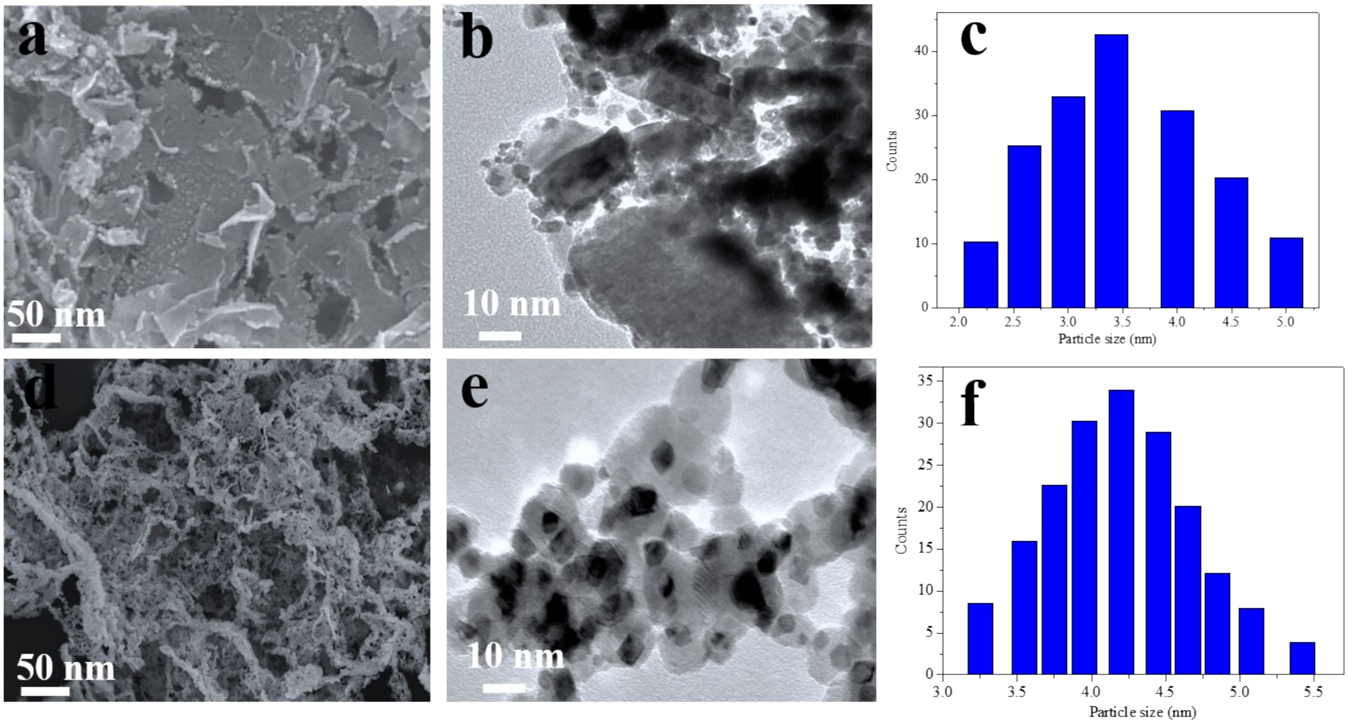

SFig. 3 FESEM, TEM images of $Co_{0.6}Ni_{0.4}$/GO and rGO (a, b), $Co_{0.4}Ni_{0.6}$/GO and rGO (d, e), and (c) and (f) are the average particle size distribution of the $Co_{0.6}Ni_{0.4}$/GO and rGO and $Co_{0.4}Ni_{0.6}$/GO and rGO, respectively.

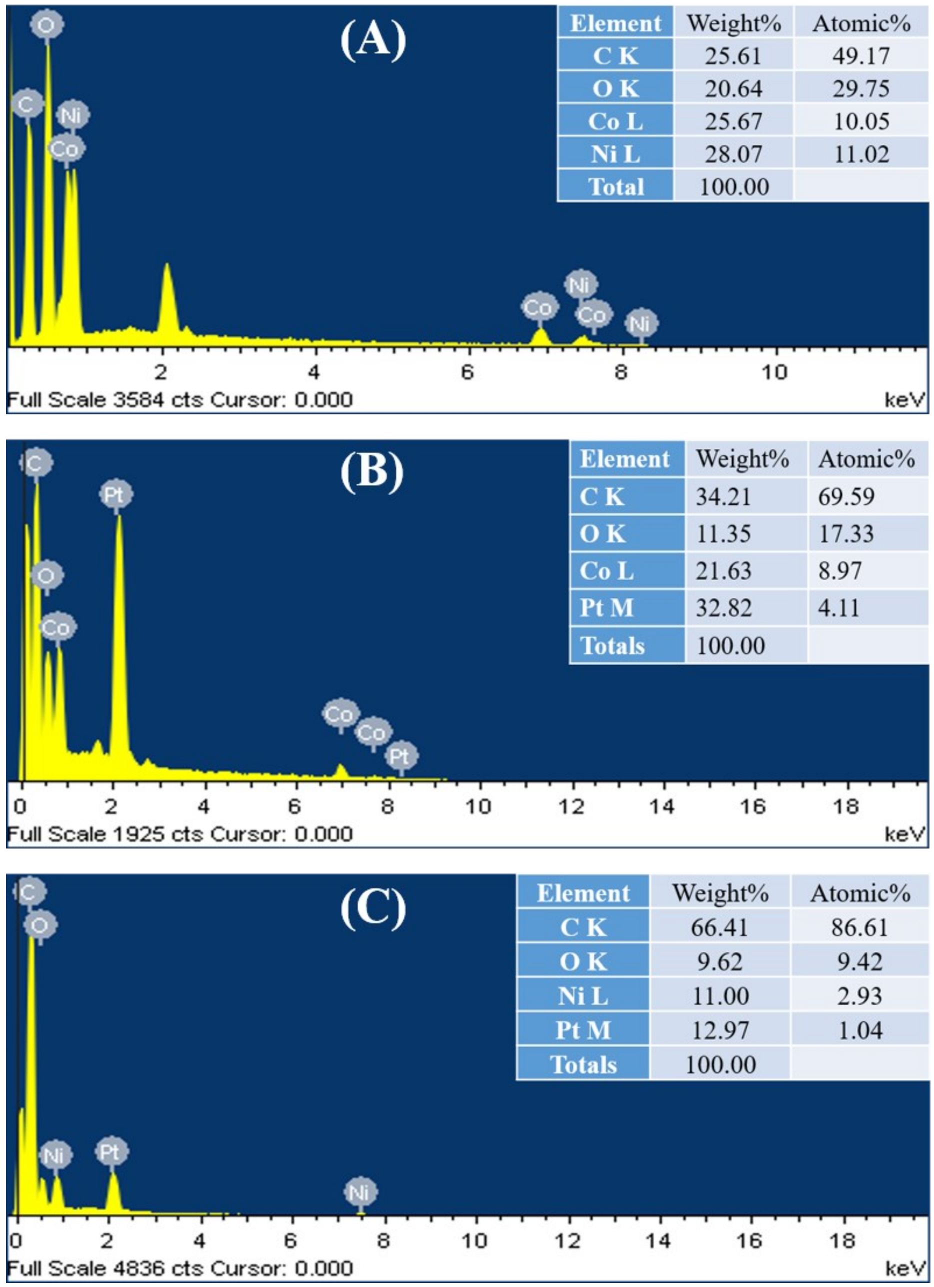

Element	Weight%	Atomic%
C K	25.61	49.17
O K	20.64	29.75
Co L	25.67	10.05
Ni L	28.07	11.02
Total	100.00	

Element	Weight%	Atomic%
C K	34.21	69.59
O K	11.35	17.33
Co L	21.63	8.97
Pt M	32.82	4.11
Totals	100.00	

Element	Weight%	Atomic%
C K	66.41	86.61
O K	9.62	9.42
Ni L	11.00	2.93
Pt M	12.97	1.04
Totals	100.00	

SFig. 4 EDX spectra of the (a) CoNi/GO and rGO, (b) CoPt/GO and rGO, and (c) NiPt/GO and rGO NPs.

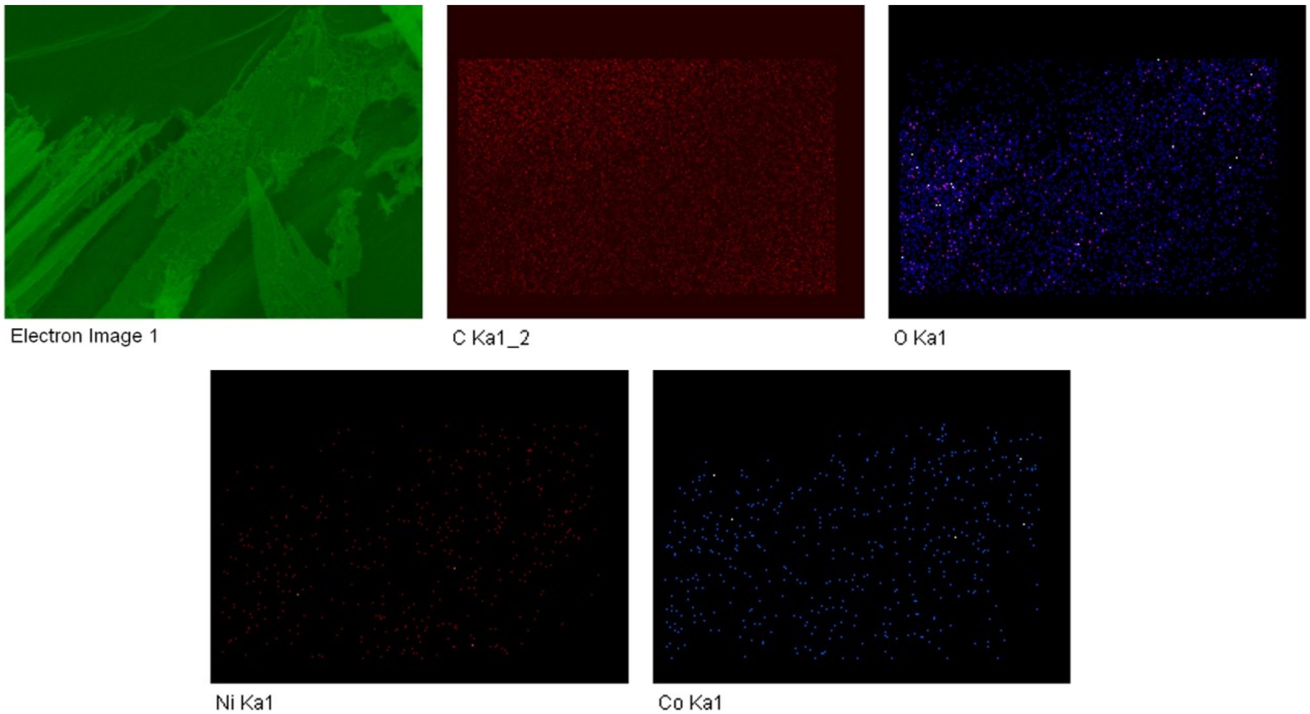

SFig. 5 FESEM and EDX mapping images of the NiCo/GO and rGO NPs.

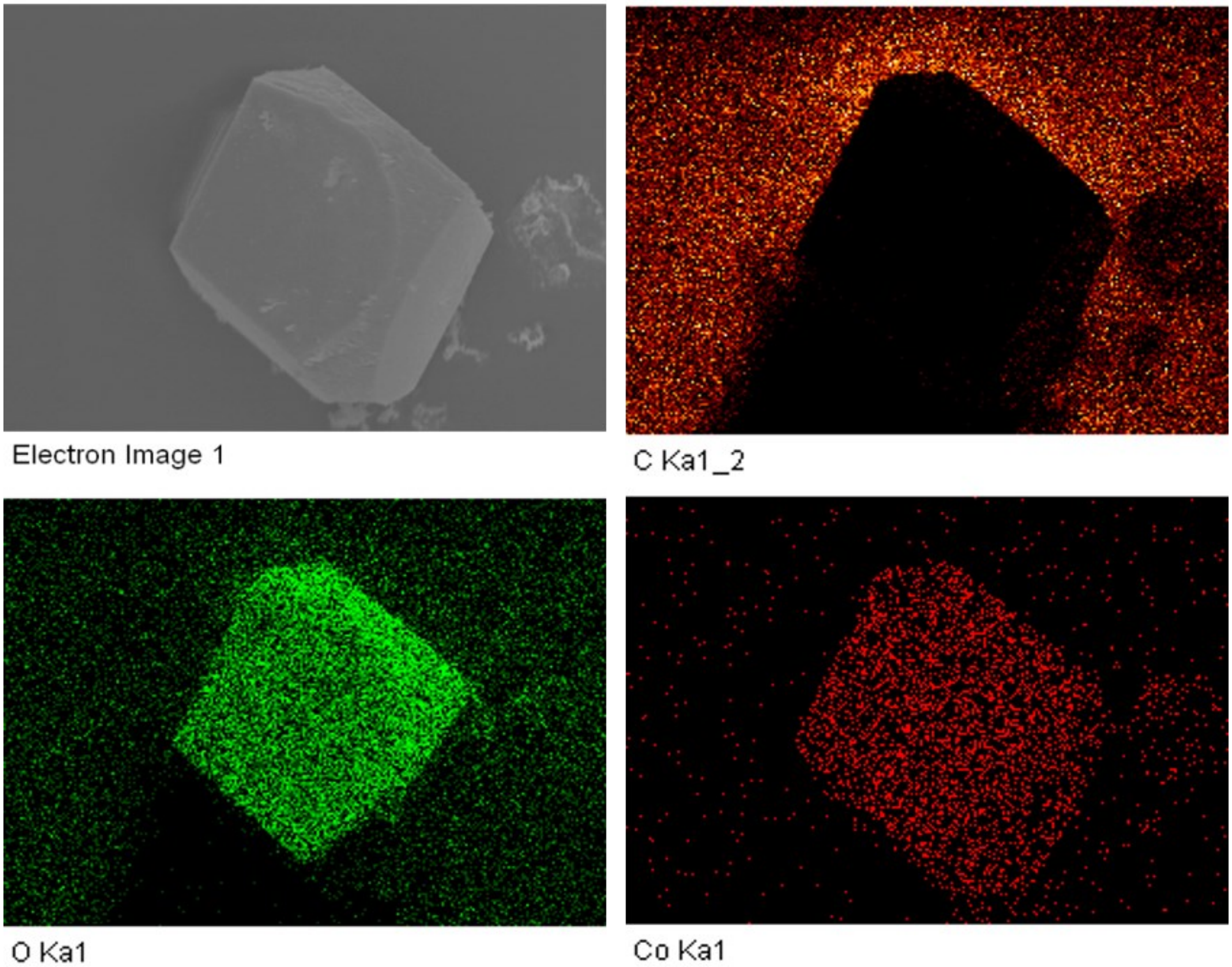

SFig. 6 FESEM and EDX mapping images of the Co/GO NPs.

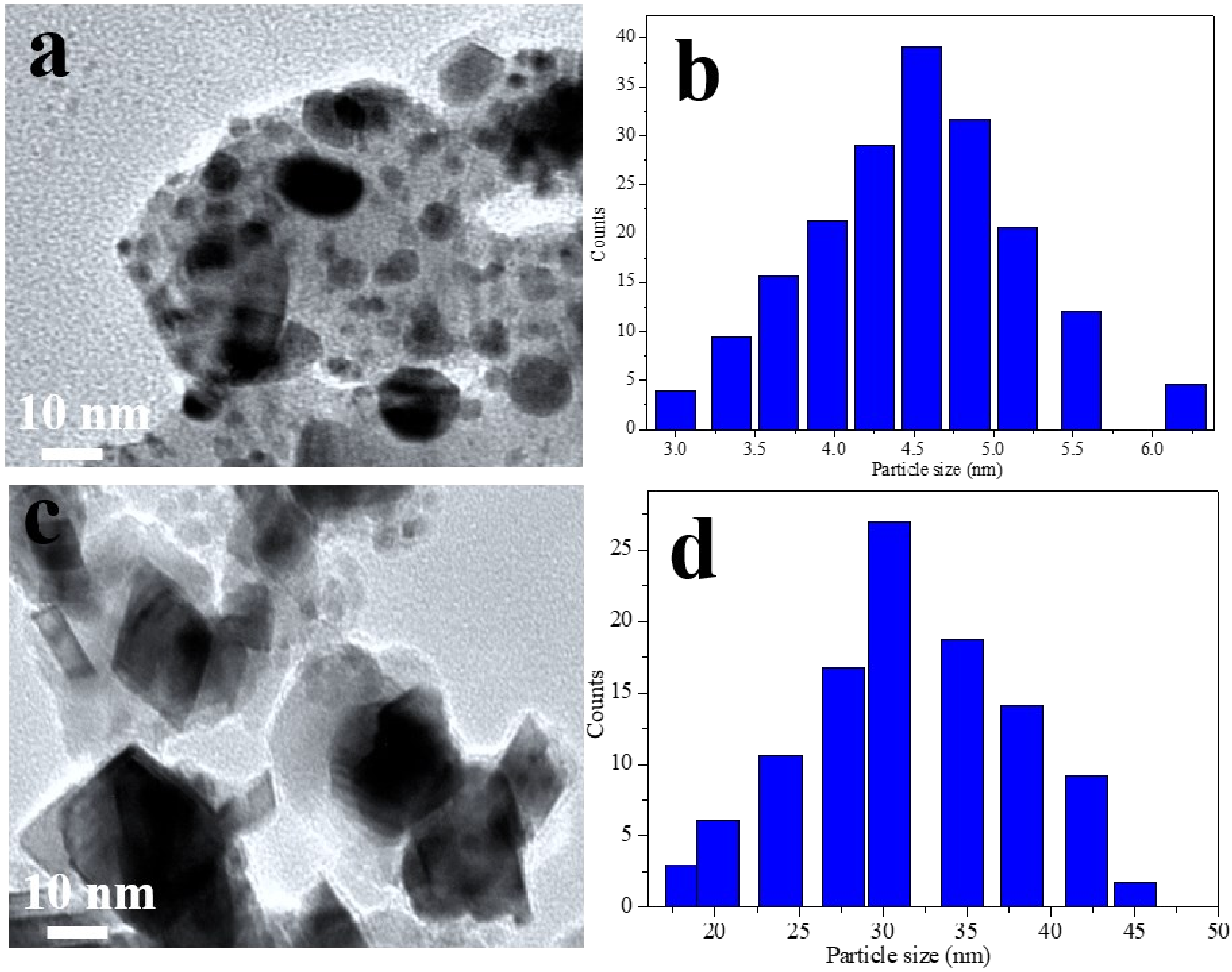

SFig. 7 TEM images and the corresponding SAED patterns of (a) Pt/GO and (c) Co/GO, particle size distribution of the (b) Pt/GO and (d) Co/GO, respectively.

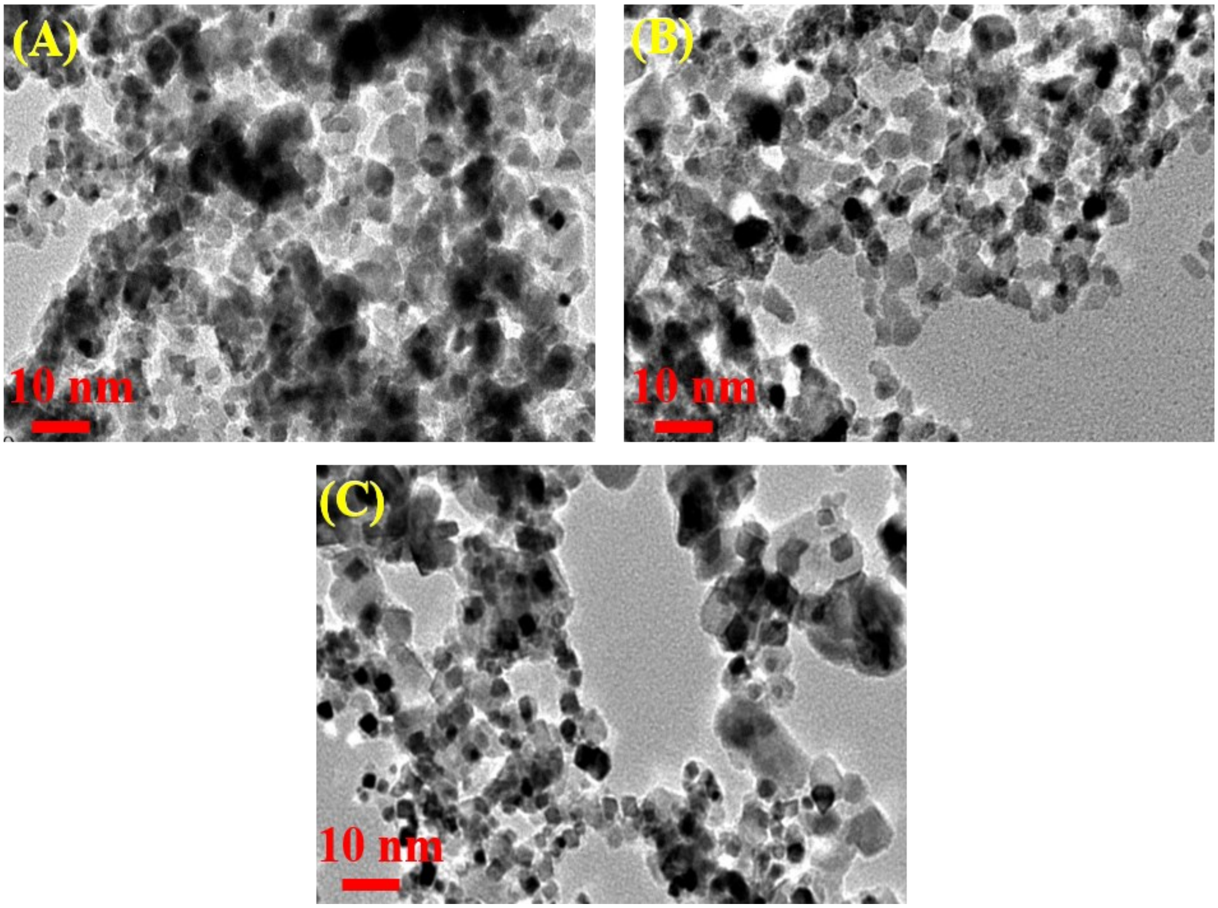

SFig. 8 TEM images of (a) NiPt/Al_2O_3, NiPt/SiO_2 and (c) CoNi/Al_2O_3.

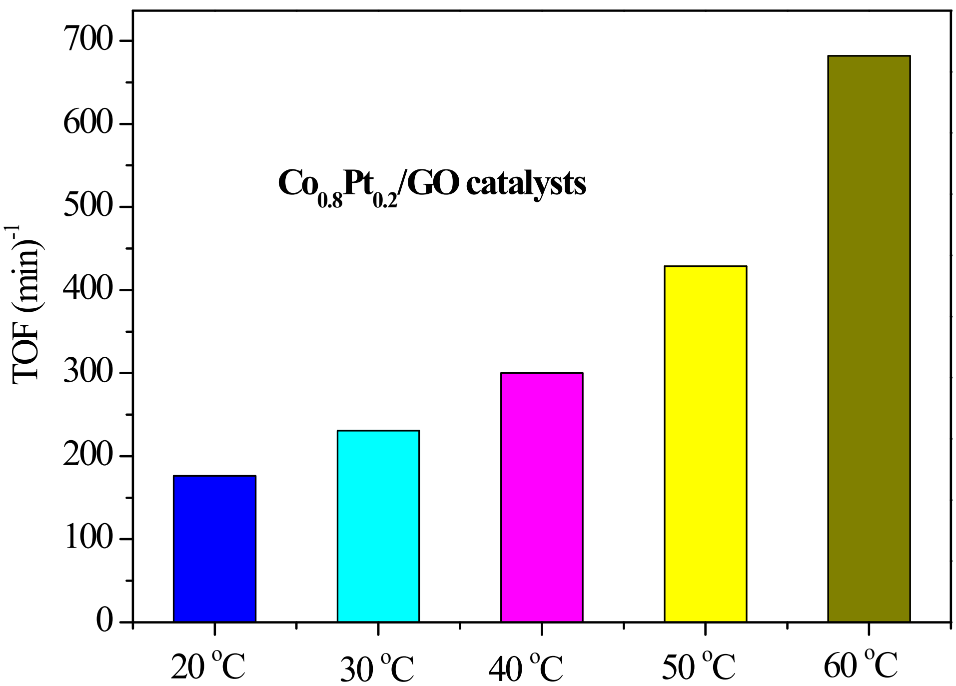

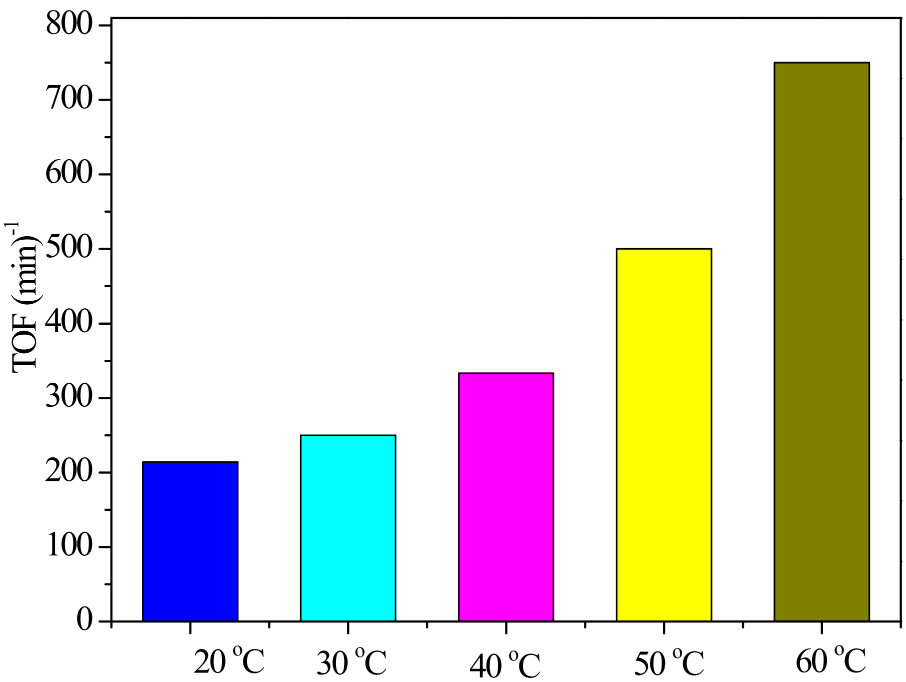

SFig. 9 shows the TOF values for aqueous AB solution hydrolysis at different temperatures (20 ^{o}C to 60 ^{o}C) (metal/AB = 0.04).

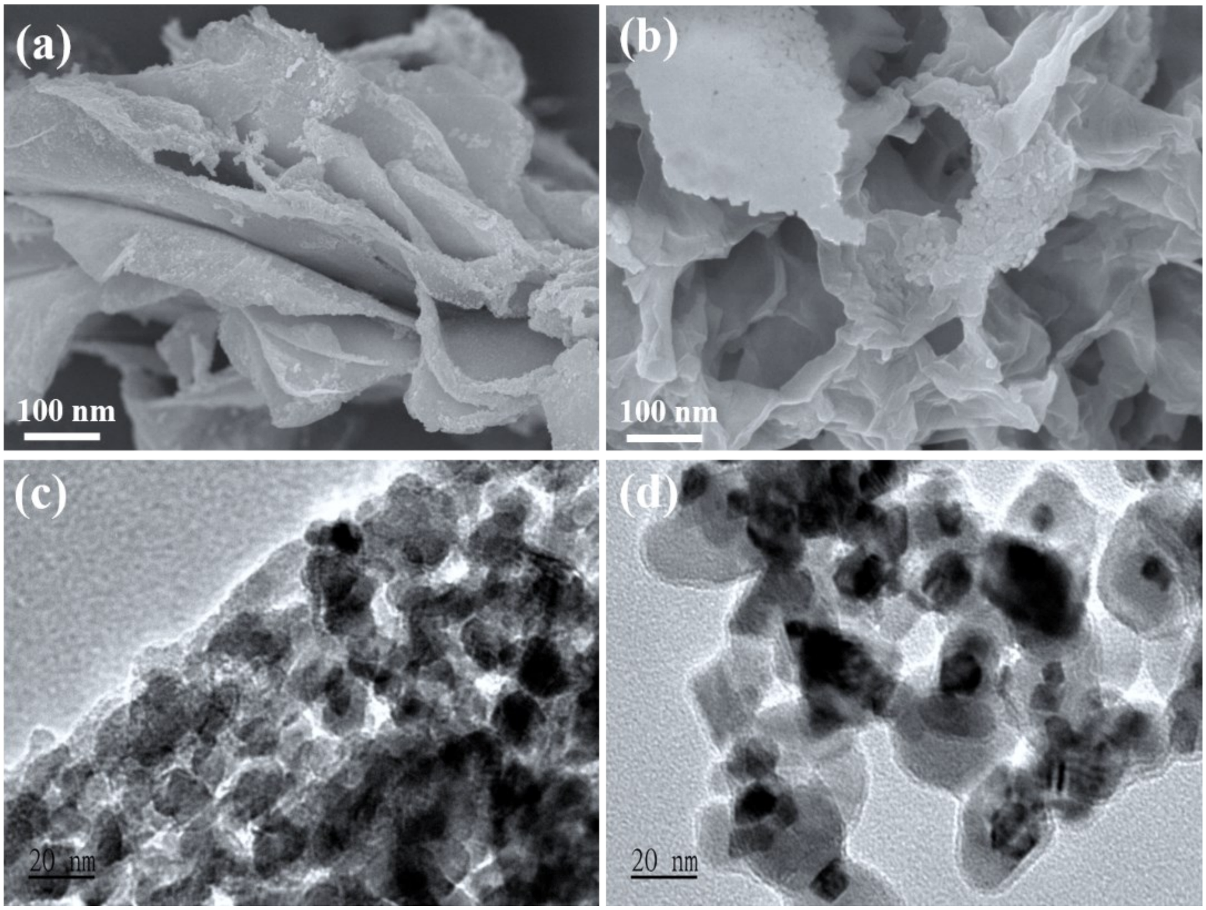

SFig. 10 (a,c) SEM and TEM images of $Ni_{0.8}Pt_{0.2}$/GO and rGO (b,d), $Co_{0.8}Pt_{0.2}$/GO and rGO nano catalyst after the stability test.

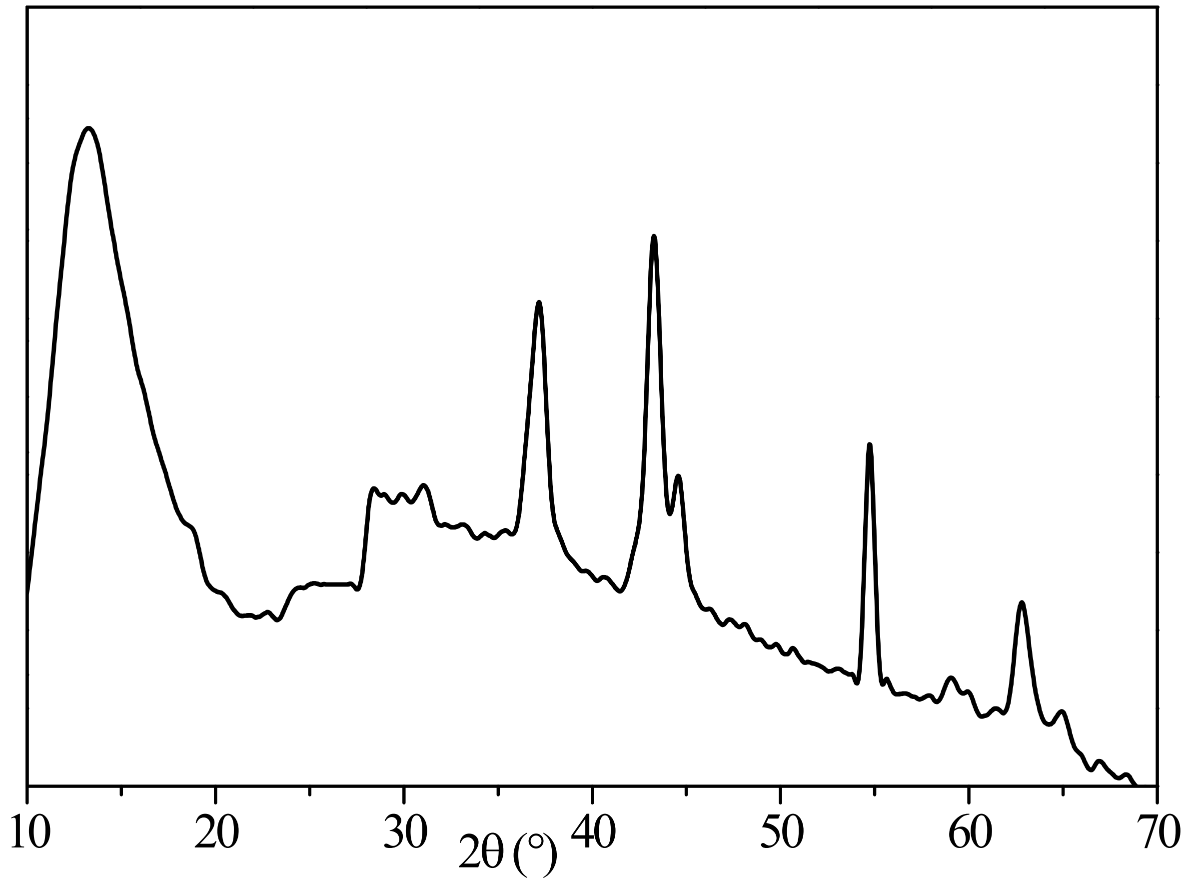

SFig. 11 X-ray diffraction patterns of $Ni_{0.8}Pt_{0.2}$/GO and rGO NPs after the durability test.

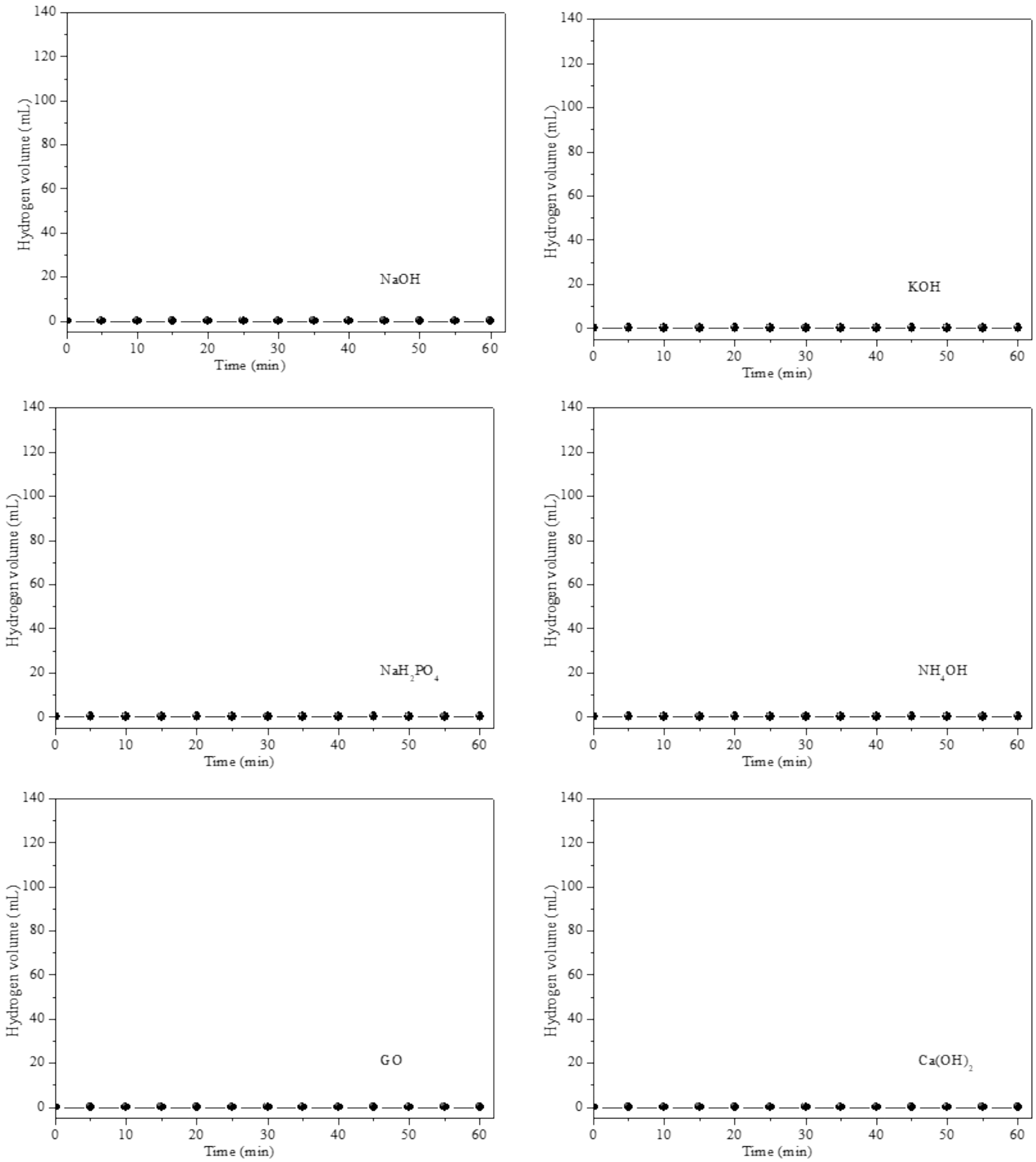

SFig. 12 Hydrogen generation from AB hydrolysis (5 mL) in the presence of 1 M (a) NaOH, (b) KOH, (c) NaH_2PO_4, (d) NH_4OH, (e) GO, and (f) $Ca(OH)_2$ at 25 ^oC.

No hydrogen generation is observed for NaOH, KOH, NaH_2PO_4, NH_4OH, GO, and $Ca(OH)_2$ toward AB hydrolysis in the absence of $Co_{0.8}Pt_{0.2}$ NPs, suggesting that these additives have no catalytic activity for AB hydrolysis.

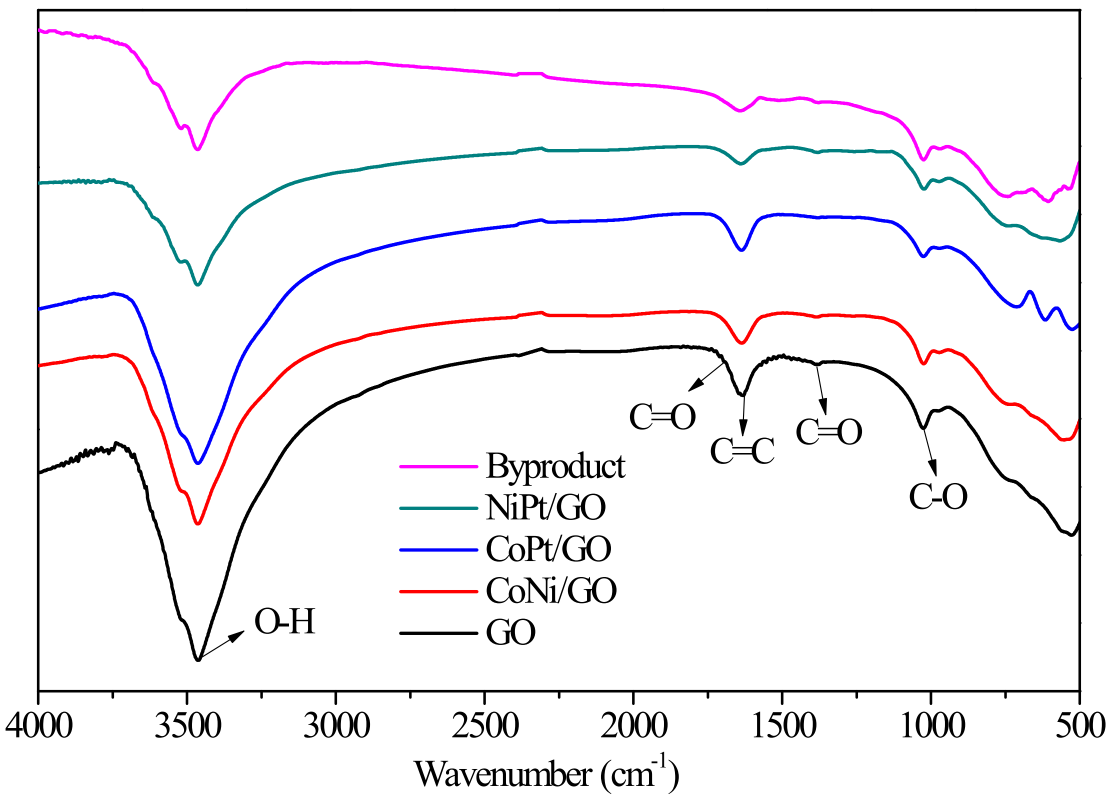

SFig. 13 FT-IR spectra of GO and metal-doped GO and rGO (M-Ni, Co, Pt).

SFig. 13 demonstrates the FT-IR spectra of GO and M-doped GO and rGO (M-Ni, Co, Pt). It can be seen that many oxygen functional groups exist on the GO Nano-sheet. The FT-IR absorption peaks of GO characterizes the presence of different existing oxygen functional groups such as O-H stretch from the carboxylic group at 3464 cm^{-1}. The absorption peak at 1709 cm^{-1} shows the existence of C=C, and the peaks at 1633 cm^{-1} attributed to the C=O stretching of carbonyl group, the peaks at 1382 cm^{-1} appearances the existence of –COO^- group and the peak at 1033 cm^{-1} characterizes the occurrence of -C-OH, respectively. Subsequently reduction of the graphene oxide (GO), some oxygen existing functional groups were disregarded, only a weak O–H carboxylic functional groups were existing in the metal-doped GO and rGO.

STable 1. The catalysts composition determined by inductively coupled plasma atomic emission spectroscopic (ICP-AES).

S.No	Catalysts	Co (%)	Ni (%)	Pt (%)
1.	Co/GO	1.35	-	-
2.	Ni/GO	2.04	-	-
3.	Pt/GO	1.87	-	-
4.	$Co_{0.4}Ni_{0.6}$/GO	1.46	5.24	-
5.	$Co_{0.6}Ni_{0.4}$/GO	2.84	3.02	-
6.	$Co_{0.8}Pt_{0.2}$/GO and rGO	4.21	-	2.10
7.	$Ni_{0.8}Pt_{0.2}$/GO and rGO	-	4.34	2.12

STable 2 Catalytic activity in terms of TOF of the graphene oxide supported metal-based catalysts for AB hydrolytic dehydrogenation.

S.No	Catalysts	H_2 (mole)	*t* (min)	TOF (min^{-1})
1.	$Co_{0.6}Ni_{0.4}$/GO	6	2.4	100.02
2.	$Co_{0.4}Ni_{0.6}$/GO	6	1.6	107.14
3.	$Co_{0.9}Pt_{0.1}$/GO	6	1.8	83.34
4.	$Ni_{0.8}Pt_{0.2}$/GO and rGO	6	0.50	214.28
5.	$Co_{0.8}Pt_{0.2}$/GO and rGO	6	0.60	230.76
6.	Ni/GO	5.9	4.6	53.57
7.	Co/GO	6	2.7	31.25
8.	Pt/GO	6	3.1	45.45

STable 3 Catalytic activity in terms of TOF of the reported metal-based catalysts for AB hydrolytic dehydrogenation.

S. No	Catalysts	*n*metal/*n*AB	*t* (min)	nH_2/nAB	TOF $(min)^{-1}$	Activation Energy (*Ea*)	References
1.	$Ni_{0.9}Mo_{0.1}$/Graphene	0.05	0.9	3	66.7	-	1
2.	$Ni_{0.9}Cr_{0.1}$/Graphene	0.05	3.5	3	17.1	-	1
3.	$Ni_{0.7}Co_{1.3}P$/rGO	0.026	10.4	3	109.4	-	2
4.	Pd-rGO	0.04	12.5	3	6.25	51	3
5.	Pd/C	0.02	80	3	1.9	-	4
6.	Ag@Co/Graphene	0.05	5	3	10.24	20.03	5
7.	AuCo@MIL-101	0.017	13	3	25.7	34	6
8.	Ag@CoFe/Graphene	0.05	10	3	8.27	32.79	7
9.	Pd@Co/Graphene	0.02	3.5	3	40.9	30.3	8
10.	$Ni_{0.8}Pt_{0.2}$/GO and rGO	0.04	0.50	6	214.28	23.94	Current work
11.	$Co_{0.8}Pt_{0.2}$/GO and rGO	0.04	0.60	6	230.76	23.60	Current work
12.	$Co_{0.4}Ni_{0.6}$/GO	0.04	1.6	6	107.14	-	Current work
13.	Pd/γ-Al_2O_3	0.018	120	3	1.39	-	9
14.	Pd/graphene aerogel	0.056	5.5	3	9.70	30.82	10

References

1 Q. Yao, Z. H. Lu, W. Huang, X. Chen and J. Zhu, *J. Mater. Chem. A*, 2016, **4**, 8579-8583.

2 C. C. Hou, Q. Li, C. J. Wang, C. Y. Peng, Q. Q. Chen, H. F. Ye and Y. Chen, *Energy Environ. Sci*., 2017, **10**, 1770-1776.

3 P. Xi, F. Chen, G. Xie, C. Ma, H. Liu, C. Shao and Z. Zeng, *Nanoscale*, 2012, **4**, 5597-5601.

4 P. V. Ramachandran and P. D. Gagare, *Inorg. Chem*., 2007, **46**, 7810-7817.

5 L. Yang, W. Luo and G. Cheng, *ACS Appl. Mater. Interfaces*, 2013, **5**, 8231-8240.

6 O. Metin and S. Ozkar, *Int. J. Hydrogen Energ*., 2011, **36**, 1424-1432.

7 L. Yang, J. Su, W. Luo and G. Cheng, *Int. J. Hydrogen Energ*., 2014, **39**, 3360-3370.

8 J. Wang, Y. L. Qin, X. Liu and X. B. Zhang, *J. Mater. Chem*., 2012, **22**, 12468-12470.

9 Q. Xu and M. Chandra, *J. Alloys Comp*., 2007, **446**, 729-732.

10 X. K. Tian, C. Yang, Z. X. Zhou, X. W. Liu, Y. Li, *Int. J. Hydrogen Energ*., 2016, **41**, 15225-15235.